2022 IEEE 95th Vehicular Technology Conference (VTC2022-Spring) | 978-1-6654-8243-1/22/$31.00 ©2022 IEEE | DOI: 10.1109/VTC2022-Spring54318.2022.9860409

Emission-aware Resource Optimization Framework for Backscatter-enabled Uplink NOMA Networks

Muhammad Ali Jamshed*, Wali Ullah Khan†, Haris Pervaiz‡, Muhammad Ali Imran*, and Masood Ur-Rehman*

* James Watt School of Engineering, University of Glasgow, Glasgow, U.K
† Interdisciplinary Center for Security, Reliability and Trust (SnT),
University of Luxembourg, 1855 Luxembourg City, Luxembourg
‡ School of Computing and Communications, Lancaster University, Lancaster, U.K
Email: {muhammadali.jamshed,masood.urrehman,muhammad.imran}@glasgow.ac.uk,
waliullah.khan@uni.lu, h.b.pervaiz@lancaster.ac.uk

***Abstract*—In the last decade, a sharp surge in the number of user proximity wireless devices (UPWDs) has been observed. This has increased the level of electromagnetic field (EMF) exposure of the users substantially and hence, the possible physiological effects. Ambient backscatter communications (ABC) has appeared to be a promising solution to reduce the power consumption of UPWDs by converting ambient radio frequency (RF) signals into useful signals while non-orthogonal multiple access (NOMA) is a compelling multiplexing scheme for enhanced spectral efficiency. This paper utilises a novel combination of ABC and NOMA to reduce the EMF in the uplink of wireless communication systems. This contemporary approach of EMF-aware resource optimization is based on k-medoids and Silhouette analysis. To curtail the uplink EMF, a power allocation strategy is also derived by converting a non-convex problem to a convex one and solving accordingly. The numerical results exhibit that the proposed ABC, NOMA, and unsupervised learning based scheme achieves a reduction in the EMF by at least 75% in comparison to the existing solutions.**

***Index Terms*—Electromagnetic field (EMF), ambient backscatter communications (ABC), non-orthogonal multiple access (NOMA), unsupervised learning, convex optimization.**

I. Introduction

The rapid growth of wireless communication has increased the number of user proximity wireless devices (UPWDs). To accommodate this increase in UPWDs, capacity has to grow by 1,000 folds. This capacity expansion will partially be met by densifying the wireless infrastructure [1]. This densification will increase the levels of electromagnetic field (EMF) exposure significantly. Although, the literature does not provide strong evidence of severe short term impacts of EMF on human health, the International Agency for Research on Cancer (IARC) and World Health Organization (WHO) have classified the EMF waves from UPWDs as carcinogenic to humans [2]. Moreover, the upsurge in UPWDs could possibly increase the long term health hazards as well [3]. To minimize the health effects of EMF, the UPWDs must comply with by International Commission on Non-Ionizing Radiation Protection (ICNIRP) (at International level) and Federal Communication Commission (FCC) (in the USA) exposure limits and regulations [4]. However, it is interesting to note that FCC consumer guidelines state; "FCC approval does not indicate the amount of EMF exposure consumers experience during normal use of the device" [5].

Use of non-orthogonal multiple access (NOMA) in modern wireless communication networks has proven to be an effective multiplexing strategy for augmented spectral efficiency and massive connectivity. There are two variants of NOMA, i.e., code-domain NOMA (CD-NOMA) and power domain non-orthogonal multiple access (PD-NOMA) and for the scope of this paper, we have focused on the latter [6]. In PD-NOMA, the UPWDs having a difference in channel properties are allocated to the same sub-carrier. The UPWDs sharing a similar resource block are multiplexed based on different power levels by employing superposition coding technique at the transmitter side and are decoded using successive interference cancellation (SIC) at the receiver end [7].

The upsurge in data requirements has significantly increased the energy needs of UPWDs that directly impact the amount of EMF absorbed by a UPWDs user. The use of ambient backscatter communications (ABC) has emerged as a promising solution to overcome the issues related to energy consumption [8]. The ABC uses existing radio frequency (RF) signals and can provide a path for data transmission between the source and the destination. The ABC can reflect the RF signals towards the intended UPWDs without altering any oscillatory circuity, hence, maximizing the energy efficiency of UPWDs [9]. These classical properties of PD-NOMA and ABC provide an effective road map to reduce the amount of EMF absorbed by UPWDs users, while maintaining quality of service (QoS).

A. Motivation and Contributions

A limited amount of work is available in the literature on reducing the amount of EMF in the uplink of a wireless system. In [10], a heuristic approach is adopted to reduce the EMF in the uplink of orthogonal frequency division multiple access (OFDMA) based cellular system, while incorporating the classical definition of exposure dose metric (EMF over time). In [11] the similar dose metric is utilized, to propose a machine learning (ML)-based uplink resource allocation scheme to reduce the EMF in the uplink of PD-NOMA system.

Authorized licensed use limited to: University of Luxembourg. Downloaded on January 03,2023 at 12:37:27 UTC from IEEE Xplore. Restrictions apply.

In this work, a new scheduling framework that relies on ABC, PD-NOMA, and ML technologies to reduce the EMF in the uplink of wireless systems is proposed. In comparison to other well-known EMF reduction strategies, the proposed framework reduces the EMF exposure by an equitable percentage. The ABC further improves the channel gain between UPWDs and the base station (BS), hence helping to further reduce the EMF. The k-medoids is used to group UPWDs into different clusters, where the number of clusters is found using Silhouette analysis. To the best of authors' knowledge, this is the first work that have relied on ABC, PD-NOMA, and ML to minimize the uplink EMF. The contributions of this study are summarized as follows:

- We have formulated a PD-NOMA based multi-user EMF scheduling scheme. In comparison with [11], we have incorporated ABC, which makes the design more challenging but provides an opportunity to achieve higher reductions in the EMF.
- In comparison with [11], we have used k-medoids instead of k-means for the user grouping. In comparison to k-means, k-medoids is more robust, less complex, and takes less time to converge [12]. Moreover, in comparison with [11], and instead of relying on multiple methods, i.e., F-test and elbow method, we have used Silhouette analysis to find the number of users per sub-carrier. Lastly, the power allocation is carried out in a EMF-aware manner.
- The Monte Carlo types of simulations are used to validate the performance of proposed optimization framework. In comparison to [10] and [11], the proposed ABC, PD-NOMA and ML based optimization framework reduces the EMF by at least 82% and 75%, respectively.

The remainder of the paper is organized as follows: the system model and the problem formulation is provided in Section II, which shows mathematical framework and the scenario considered to design the ABC and PD-NOMA based EMF-aware technique. Section III explains the proposed EMF-aware resource and power allocation strategies. The simulation carried out to study the superiority of our proposed technique over the similar strategies is provided in Section IV. Finally, the conclusion are drawn in Section V.

II. System Model

A single cell scenario of PD-NOMA and ABC based communication system is shown in Fig. 1. The single cell of radius R_s is equipped with a single BS and U UPWDs incorporated with a single antenna and are able to communicate with the BS. To facilitate the communication between UPWDs and the BS, b, backscatter tags are available within the coverage area of BS. The system bandwidth W is equally divide into O sub-carriers such that, $w = W/|O|$. Based on NOMA property, $U_{o,\hat{t}}$ users can be allocated to a o sub-carrier at a given $\hat{t}$ time slot, where $U_{o,\hat{t}} > 1$. Since, we have considered an uplink scenario, a backscatter tag b also receives RF signal over o sub-carrier, harvest its own energy, modulate its own information, and

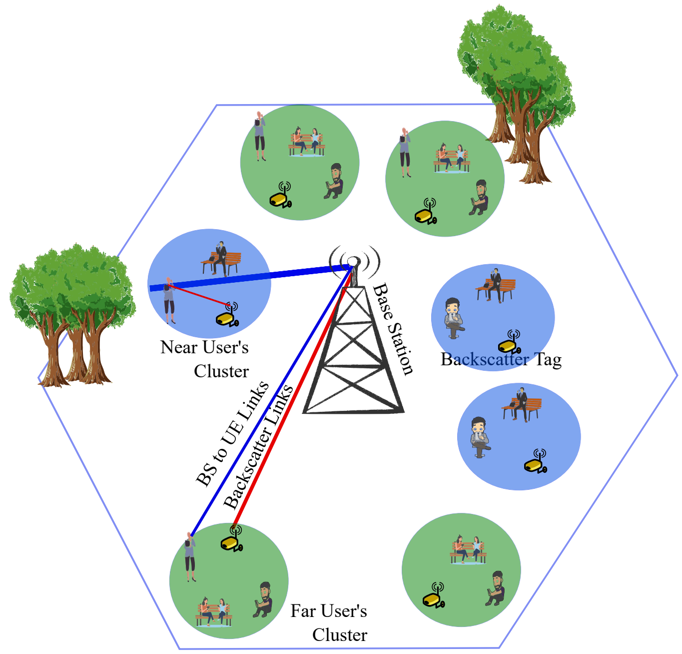

Fig. 1. Illustration of the system model.

reflect it towards BS. Thus, the received signal at the BS can be expressed as:

$$y_{o,\hat{t}} = \sum_{u=1}^{U_{o,\hat{t}}} \Big(\sqrt{p_{u,o,\hat{t}} g_{u,o,\hat{t}}} x_{u,o,\hat{t}} + \sqrt{p_{u,o,\hat{t}} \xi_b g^u_{b,o,\hat{t}} g^b_{u,o,\hat{t}}} z_{u,o,\hat{t}} x_{u,o,\hat{t}} \Big) + \omega_{o,\hat{t}}, \tag{1}$$

here $p_{u,o,\hat{t}}$ represents the transmit power of the u^{th} UPWD at $\hat{t}$ time slot and o subcarrier, $g_{k,o,\hat{t}}$ represents the channel gain between the BS and the u^{th} UPWD at $\hat{t}$ time slot and o sub-carrier, $x_{u,o,\hat{t}}$ is the information signal of u^{th} UPWD at $\hat{t}$ time slot and o sub-carrier. Accordingly, ξ_b is the reflection coefficient of backscatter b, $g^u_{b,o,\hat{t}}$ represents the channel gain between u^{th} UPWD and backscatter b at $\hat{t}$ time slot and o sub-carrier, $g^b_{u,o,\hat{t}}$ denotes the channel gain between backscatter tag b and BS at $\hat{t}$ time slot and o sub-carrier, and $\omega_{o,\hat{t}}$ is the additive white Gaussian noise (AWGN) with a zero mean and variance of σ^2, at $\hat{t}$ time slot and o sub-carrier. In NOMA, the interference occurs due to the multiplexing of different users data on a single sub-carrier. The u^{th} user multiplexed on sub-carrier o experiences the following total interference:

$$\bar{I}_{u,o,\hat{t}} = \sum_{l=1, l\neq u}^{U_{o,\hat{t}}} p_{l,o,\hat{t}} (g_{l,o,\hat{t}} + \xi_b g^l_{b,o,\hat{t}} g^b_{l,o,\hat{t}}). \tag{2}$$

In order to perform decoding of the users multiplexed together, the SIC is executed at the signal receiving side. In the uplink scenario of PD-NOMA, firstly, the users with best channel gain are demultiplexed, which is then followed by decoding of the worst channel gain users [13]. In PD-NOMA, the multiplexing strategy highly depends on the ability of SIC to successfully decode the multiplexed signal [14]. This can be achieved if

Authorized licensed use limited to: University of Luxembourg. Downloaded on January 03,2023 at 12:37:27 UTC from IEEE Xplore. Restrictions apply.

the ratio of received signal to residual interference of user u on sub-carrier o of $\hat{t}$ time slot meets the following condition:

$$p_{u,o,\hat{t}}(g_{u,o,\hat{t}} + \xi_b g^u_{b,o,\hat{t}} g^b_{u,o,\hat{t}})/I_{u,o,\hat{t}} \geq \zeta, \tag{3}$$

the reference threshold $\zeta \geq 1$, where:

$$I_{u,o,\hat{t}} = \sum_{l=\pi^{-1}(u)+1}^{U_{o,\hat{t}}} p_{\pi(l),o,\hat{t}}(g_{\pi(l),o,\hat{t}} + \xi_b g^{\pi(l)}_{b,o,\hat{t}} g^b_{\pi(l),o,\hat{t}}). \tag{4}$$

Using Shannon formula, the transmitted number of bits over a τ duration of time slot $\hat{t}$ and sub-carrier o by a user u is expressed as:

$$bt_{u,o,\hat{t}(\alpha,p)} = w\tau\, \alpha_{u,o,\hat{t}} \log_2\left(1 + \frac{p_{u,o,\hat{t}}(g_{u,o,\hat{t}} + \xi_b g^u_{b,o,\hat{t}} g^b_{u,o,\hat{t}})}{\sigma^2 + I_{u,o,\hat{t}}}\right), \tag{5}$$

where, $\alpha_{u,o,\hat{t}}$ is sub-carrier allocation index and w is the bandwidth of each sub-carrier. The level of EMF in the uplink of a single user u is defined as [15]:

$$E_u(\alpha, p) = \frac{\mathrm{SAR}_u}{\hat{T} P^{\mathrm{ref}}} \tau \left(\hat{p}_u(\hat{T}) + \sum_{\hat{t}=1}^{\hat{T}} \sum_{o=1}^{O} \alpha_{u,o,\hat{t}} p_{u,o,\hat{t}}\right), \tag{6}$$

here, P^{ref} is reference incident power used to estimate specific absorption rate (SAR), $\hat{T}$ is total number of time slots, and $\hat{p}_u(\hat{T})$ is the signalling power. The SAR and $\hat{p}_u(\hat{T})$ can be computed as discussed in [3].

A. Problem Formulation

In this work, the objective is to reduce the total uplink EMF while considering a PD-NOMA and ABC enabled cellular framework. The optimization problem is formulated in the form of mathematical expressions and is defined as follows:

$$(\mathrm{OP}) \min_{p,\alpha} \quad E(\alpha, p) = \sum_{u=1}^{U} E_u(\alpha, p),$$

s.t:

$$\begin{aligned}
&(C1): \sum_{\hat{t}=1}^{\hat{T}} \sum_{o=1}^{O} bt_{u,o,\hat{t}}(\alpha, p) = Bt_u, \forall u \\
&(C2): \sum_{o=1}^{O} \alpha_{u,o,\hat{t}} p_{u,o,\hat{t}} \leq P_u^{\max} \quad \forall u, \forall \hat{t}, \\
&(C3): \alpha_{u,o,\hat{t}}(p_{u,o,\hat{t}}(g_{u,o,\hat{t}} + \xi_b g^u_{b,o,\hat{t}} g^b_{u,o,\hat{t}})/I_{u,o,\hat{t}}) \geq \zeta \quad \forall u, \forall o, \forall \hat{t}, \\
&(C4): \sum_{u=1}^{U} \alpha_{u,o,\hat{t}} \leq U_{o,\hat{t}} \quad \forall o, \forall \hat{t}, \\
&(C5): 0 \leq \xi_b \leq 1 \quad \forall b,
\end{aligned} \tag{7}$$

where, the total EMF absorbed by U users over $\hat{T}$ time slots is expressed by objective function $E(\alpha, \mathbf{p})$ in (OP). The constraint $(C1)$ ensures the QoS of each user. The $(C2)$ constraint is related to the maximum power limit $P_u^{\max}$ of each user. The $(C3)$ constraint is related to the successful implementation of SIC. The constraint $(C4)$ reflects the maximum allowable users on a single sub-carrier. Finally, the constraint $(C5)$ controls the reflection of backscatter tags. The binary nature of $\alpha_{u,o,\hat{t}}$ and non-affine nature the $(C1)$ constraint, makes the problem non-convex [16]. A standard relaxation procedure needs to be applied to overcome the binary nature of $\alpha_{u,o,\hat{t}}$. This is catered by adopting a sequential sub-carrier and power allocation strategy, i.e., performing sub-carrier allocation for a fixed power and vice versa [17]. Moreover, it is assumed that the channel state information (CSI) is available by exploiting uplink pilot signals.

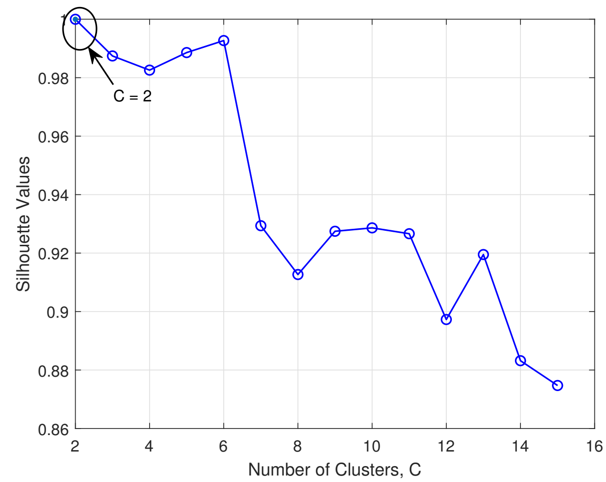

Fig. 2. Silhouette values versus C for $O = 1$, $U = 100$, and $\hat{T} = 1$.

III. Proposed Solution

A. Sub-carrier Allocation

In PD-NOMA the $U_{o,\hat{t}}$ users can be assigned to a single sub-carrier by exploiting the variations in their channel properties and are demultiplexed by using the levels of received power. The sub-carrier assignment relies on receiver capability to differentiate between power levels, which itself relies on grouping of users on same sub-carrier. In comparison to heuristic techniques, the use of clustering based ML algorithms have proven to be much effective, less complex and have a higher probability of convergence [12]. Here, similar to [11], we have used ML techniques to perform the sub-carrier allocation. However, instead of using k-means, the k-medoids based clustering is employed due to its low complexity and robustness. Moreover, instead of relying on traditional F-test and elbow methods for predicting the best number of clusters, a Silhouette analysis has been carried out. The elbow method, provides a range based on elbow criteria, hence creating ambiguities in selecting the best value of C. Whereas, the Silhouette analysis is more robust and removes such ambiguities.

Figure 2, shows the trend of Silhouette values by varying C, for $U = 100$, $O = 1$, and $\hat{T} = 1$ over a Rayleigh fading channel and path loss model defined in [18]. The clusters are formed using k-medoids. It can be observed that for $C = 2$, a Silhouette value of 1 is achieved, which corresponds to number of users that can be multiplexed on a single sub-carrier. Once a suitable value of C is selected, the sub-carrier allocation is

Authorized licensed use limited to: University of Luxembourg. Downloaded on January 03,2023 at 12:37:27 UTC from IEEE Xplore. Restrictions apply.

performed by relying on normalized channel gain, i.e., $G_{u,o,\hat{t}}$, to maintain fairness among all users.

B. Power Allocation

After the learning-based sub-carrier allocation, the power for each user needs to be allocated optimally to minimize the uplink EMF. The constraint $(C1)$ in (OP) is still non-convex and to overcome its non-linear nature, the (5) is transformed as follows:

$$p_{u,o,\hat{t}} = \frac{(2^{r_{u,o,\hat{t}}}-1)(\sigma^2+I_{u,o,\hat{t}})}{g_{u,o,\hat{t}}+\xi_b g^u_{b,o,\hat{t}} g^b_{u,o,\hat{t}}}, \tag{8}$$

and by using $p_{u,o,\hat{t}}$, the (OP) can be re-defined as follows:

$$\min_{r} \frac{\tau}{\hat{T}} \sum_{u=1}^{U} \left(\hat{p}_u(\hat{T}) + \sum_{\hat{t}=1}^{\hat{T}} \sum_{o=1}^{O} \frac{\alpha_{u,o,\hat{t}}(2^{r_{u,o,\hat{t}}}-1)(\sigma^2+I_{u,o,\hat{t}})}{(g_{u,o,\hat{t}}+\xi_b g^u_{b,o,\hat{t}} g^b_{u,o,\hat{t}})} \right),$$

s.t:

$$\begin{aligned}
&(C6): w\tau \sum_{\hat{t}=1}^{\hat{T}} \sum_{o=1}^{O} \alpha_{u,o,\hat{t}} r_{u,o,\hat{t}} = Bt_u, \\
&(C7): \sum_{o=1}^{O} \frac{\alpha_{u,o,\hat{t}}(2^{r_{u,o,\hat{t}}}-1)(\sigma^2+I_{u,o,\hat{t}})}{(g_{u,o,\hat{t}}+\xi_b g^u_{b,o,\hat{t}} g^b_{u,o,\hat{t}})} \le P^{\max}_u, \\
&(C8): \alpha_{u,o,\hat{t}}((2^{r_{u,o,\hat{t}}}-1)(\sigma^2+I_{u,o,\hat{t}})/I_{u,o,\hat{t}}) \ge \zeta,
\end{aligned} \tag{9}$$

here, the spectral efficiency of u user is defined as $r_{u,o,\hat{t}} = bt_{u,o,\hat{t}}/(w\tau)$. In comparison to (OP), (9), as a function of $\mathbf{r}$ is affine. Since, the problem defined in (9) is convex, its Lagrangian can be found easily, defined as follows:

$$r_{u,o,\hat{t}} = \max\left(0, \log_2 \chi + \log_2\left(\frac{w(g_{u,o,\hat{t}}+\xi_b g^u_{b,o,\hat{t}} g^b_{u,o,\hat{t}})}{\ln(2)(\sigma^2+I_{u,o,\hat{t}})}\right)\right), \tag{10}$$

where, λ_u, $\mu_{u,\hat{t}}$ and $\delta_{u,o,\hat{t}}$ are associated Lagrange multipliers of $(C6)$, $(C7)$ and $(C8)$. The χ is expressed as:

$$\chi = \frac{\lambda^\star_u}{(1/\hat{T} - (\mu^\star_{u,\hat{t}} + \delta^\star_{u,o,\hat{t}}(g_{u,o,\hat{t}}+\xi_b g^u_{b,o,\hat{t}} g^b_{u,o,\hat{t}})/I_{u,o,\hat{t}})/\tau)}. \tag{11}$$

The equation (10) is a water-filling based solution and can be solved by employing different iterative solutions [10]. The details about sub-carrier allocation and power assignment schemes are provided in Algorithm 1.

IV. Performance Evaluation

The performance of the proposed ABC and PD-NOMA enabled scheme is validated using MATLAB simulations. The coverage radius of BS is set as $R_s = 500$ meters, where U users are randomly placed uniformly. The Rayleigh fading and the path loss model defined in [18] is used to model propagation effects. A single backscatter tag b is considered in each cluster to facilitate the communication between BS and users. We assume that the values of SAR_u and P^{ref} are constants (pertaining to FCC limits), and the number of bits is the same for all users. The $\sigma^2 = -174$ dBm/Hz, $W = 10$ MHz, $\zeta = 1$, $\xi = 1$, $P_{\max} = 0.2$ W, $\tau = 1$ ms, $\mathrm{SAR}_u = 1$ W/kg, and $P^{\mathrm{ref}} = 1$ W, are assumed. The sub-carrier and power allocation is performed using the steps defined in Algorithm 1.

In Fig. 3, a comparison of the proposed scheme with [10] and [11], is carried out by increasing the number of bits for

Algorithm 1: Low EMF learning based ABC and PD-NOMA-enabled optimization framework.

INPUT (U, $\hat{T}$, O, $g_{u,o,\hat{t}}$, $g^u_{b,o,\hat{t}}$, $g^b_{u,o,\hat{t}}$, α, ζ, SAR_u, $P^{\max}_u$, Bt_u, τ, $\hat{p}_u(\hat{T})$, σ^2, w, ξ_b, b)
Step 1: User grouping
for $C = 2 : U-1$ **do**
  Use K-mediods to cluster $\mathbf{g}_{o,\hat{t}} = [g_{1,o,\hat{t}}, \ldots, g_{U,o,\hat{t}}]$;
  Set $U_{o,\hat{t}} = C$ based on Silhouette analysis;
end for
Step 2: Sub-carrier allocation
Use $G_{u,o,\hat{t}} = g_{u,o,\hat{t}}/\hat{g}_u \ \forall u,o,\hat{t}$, where $\hat{g}_u$ is the mean channel gain.
Use max. of $G_{.,o,\hat{t}}$ within each cluster for each user.
Allocate $S = \frac{O\times\hat{T}}{U}$ sub-carrier to each user.
Step 3: Power assignment
Set $p_{u,o,\hat{t}} = P^{\max}_u/S$ to estimate initial interference;
repeat
  for $u = 1 : U$ **do**
    Estimate $r_{u,o,\hat{t}}$ using iterative water-filling and satisfying SIC constraint;
    Estimate $p_{u,o,\hat{t}}$ utilizing (8);
    Re-evaluate $I_{u,o,\hat{t}}$ utilizing (4);
    Estimate E_u utilizing (6);
  end for
until convergence
Evaluate E utilizing (OP);
OUTPUT E;

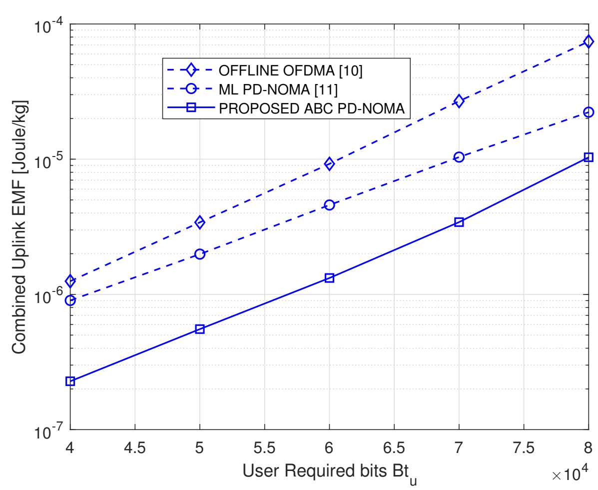

Fig. 3. Comparing combined uplink EMF against a variation in the bits for U = 15, $\hat{T}$ = 10, and O = 128.

Authorized licensed use limited to: University of Luxembourg. Downloaded on January 03,2023 at 12:37:27 UTC from IEEE Xplore. Restrictions apply.

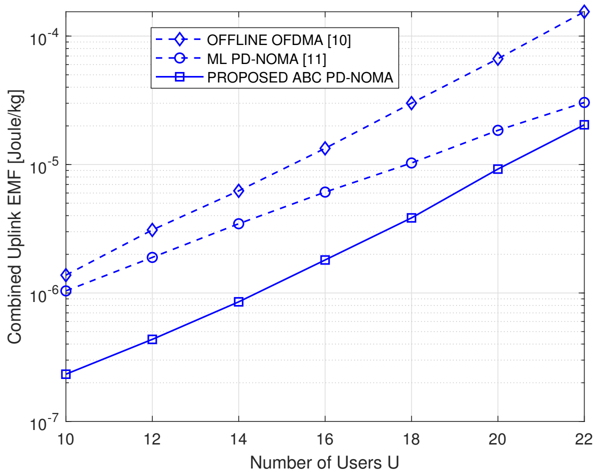

Fig. 4. Comparing combined uplink EMF against a variation in the number of users for fixed bits, time slots and sub-carriers.

$O = 128$ sub-carriers, $U = 15$ users, and $\hat{T} = 10$ time slots. A rising tendency in the EMF can be seen for increasing number of bits as each user requires more transmit power to achieve the required number of bits. In comparison to OFDMA method [10], the proposed ABC and PD-NOMA based scheme achieves 82% reduction in EMF for $Bt = 40$ kbit, as PD-NOMA possess an increase in spectral efficieny by allowing $U_{o,\hat{t}}$ users to share the same sub-carrier and the use of SIC helps to reduce the uplink power. In comparison to a similar ML-based PD-NOMA strategy [11], our scheme reduces the EMF by 75% for $Bt = 40$ kbit, as the addition of backscatter tags helps to further improve the channel quality between users and the BS.

In Fig. 4, a comparison of the proposed scheme with the techniques discussed in [10] and [11] is carried out by increasing the value of U for a fixed value of $O = 128$, $\hat{T} = 10$, and $Bt_u = 60$ kbits. An increasing trend in EMF can be seen for larger number of users as each user requires more transmit power to achieve same number of bits, while the number of allocated sub-carrier and the size of transmission window are fixed. In comparison to [10], the proposed ABC and PD-NOMA based scheme allows multiple users to share the same sub-carrier, hence providing at least 87% reduction in EMF. While comparing with the similar ML PD-NOMA scheme of [11], at least 33% reduction in the EMF is achieved, which is largely due to the addition of ABC.

V. Conclusion

A new EMF-aware resource allocation and user grouping scheme is proposed by using ML technologies for ABC and PD-NOMA based wireless systems. The k-medoids and Silhouette analysis has been used to perform user grouping and sub-carrier allocation, which is then followed by power assignment. The power assignment is performed through solving the (OP). In comparison to similar techniques, our proposed framework reduces the EMF by at least 75%. These results indicate the vast potential of this novel method and indicate its suitability to be used in modern wireless networks with significantly reduced EMF of UPWDs.

Acknowledgement

This work was supported by Innovative and Collaborative Research Grant under Pakistan UK Education Gateway (ICRG-2020) Project No. 310366 - Deforestation in Pakistan: Combating through Wireless Sensor Networks (DePWiSeN)).

References

[1] F. Boccardi, R. W. Heath, A. Lozano, T. L. Marzetta, and P. Popovski, “Five disruptive technology directions for 5G,” *IEEE communications magazine*, vol. 52, no. 2, pp. 74–80, 2014.
[2] I. A. for Research on Cancer *et al.*, “IARC classifies radiofrequency electromagnetic fields as possibly carcinogenic to humans,” *Press release*, no. 208, 2011.
[3] M. A. Jamshed, F. Heliot, and T. Brown, “A Survey on Electromagnetic Risk Assessment and Evaluation Mechanism for Future Wireless Communication Systems,” *IEEE Journal of Electromagnetics, RF and Microwaves in Medicine and Biology*, 2019.
[4] M. U. Rehman, Y. Gao, Z. W. J. Zhang, Y. Alfadhl, X. Chen, C. Parini, Z. Ying, and T. Bolin, “Investigation of on-body bluetooth transmission,” *IET Microwaves, Antennas Propagation*, vol. 4, pp. 871–880, July 2010.
[5] F. C. Commission *et al.*, “Specific absorption rate (SAR) for cell phones: what it means for you,” 2014.
[6] L. Dai, B. Wang, Z. Ding, Z. Wang, S. Chen, and L. Hanzo, “A Survey of Non-Orthogonal Multiple Access for 5G,” *IEEE Communications Surveys & Tutorials*, 2018.
[7] W. U. Khan, F. Jameel, M. A. Jamshed, H. Pervaiz, S. Khan, and J. Liu, “Efficient power allocation for noma-enabled iot networks in 6g era,” *Physical Communication*, vol. 39, p. 101043, 2020.
[8] F. Jameel, M. A. Jamshed, Z. Chang, R. Jäntti, and H. Pervaiz, “Low latency ambient backscatter communications with deep q-learning for beyond 5g applications,” in *2020 IEEE 91st Vehicular Technology Conference (VTC2020-Spring)*. IEEE, 2020, pp. 1–6.
[9] W. U. Khan, M. A. Javed, T. N. Nguyen, S. Khan, and B. M. Elhalawany, “Energy-efficient resource allocation for 6g backscatter-enabled noma iov networks,” *IEEE Transactions on Intelligent Transportation Systems*, 2021.
[10] Y. A. Sambo, M. Al-Imari, F. Héliot, and M. A. Imran, “Electromagnetic emission-aware schedulers for the uplink of OFDM wireless communication systems,” *IEEE Transactions on Vehicular Technology*, vol. 66, no. 2, pp. 1313–1323, 2016.
[11] M. A. Jamshed, F. Heliot, and T. Brown, “Unsupervised learning based emission-aware uplink resource allocation scheme for non-orthogonal multiple access systems,” *IEEE Transactions on Vehicular Technology*, 2021.
[12] T. Velmurugan and T. Santhanam, “Computational complexity between k-means and k-medoids clustering algorithms for normal and uniform distributions of data points,” *Journal of computer science*, vol. 6, no. 3, p. 363, 2010.
[13] G. D. Golden, C. Foschini, R. A. Valenzuela, and P. W. Wolniansky, “Detection algorithm and initial laboratory results using V-BLAST space-time communication architecture,” *Electronics letters*, vol. 35, no. 1, pp. 14–16, 1999.
[14] Z. Ali, G. A. S. Sidhu, M. Waqas, and F. Gao, “On fair power optimization in nonorthogonal multiple access multiuser networks,” *Transactions on Emerging Telecommunications Technologies*, vol. 29, no. 12, p. e3540, 2018.
[15] E. Conil, “D2. 4 Global wireless exposure metric definition v1,” *LexNet project*, 2013.
[16] Z.-Q. Luo and W. Yu, “An introduction to convex optimization for communications and signal processing,” *IEEE Journal on selected areas in communications*, vol. 24, no. 8, pp. 1426–1438, 2006.
[17] M. Al-Imari, P. Xiao, M. A. Imran, and R. Tafazolli, “Low complexity subcarrier and power allocation algorithm for uplink OFDMA systems,” *EURASIP Journal on Wireless Communications and Networking*, vol. 2013, no. 1, pp. 1–6, 2013.
[18] J. Wu, S. Rangan, and H. Zhang, *Green communications: theoretical fundamentals, algorithms, and applications*. CRC press, 2016.

Authorized licensed use limited to: University of Luxembourg. Downloaded on January 03,2023 at 12:37:27 UTC from IEEE Xplore. Restrictions apply.